

Rigorous Design of Reaction-Separation Processes Using Disjunctive Programming Models

Xiang Zhang^{a,b}, Zhen Song^a, Teng Zhou^{a,*}

^a Process Systems Engineering, Max Planck Institute for Dynamics of Complex Technical Systems, Sandtorstr. 1, D-39106 Magdeburg, Germany

^b Department of Chemical and Biomolecular Engineering, The Hong Kong University of Science and Technology, Hong Kong, China

** Corresponding author: zhout@mpi-magdeburg.mpg.de*

ABSTRACT

A systematic and efficient method for the rigorous design of complex chemical processes is significant in the chemical industry. In this paper, a superstructure-based optimization approach for the rigorous and simultaneous design of reaction and separation processes using generalized disjunctive programming (GDP) models is presented. In the reactor network, disjunctions for conditional reactors are introduced where the balance and reaction kinetic equations are applied only if the reactor is selected. Based on the proposed reactor disjunctions, two different reactor superstructures are developed and employed. In addition, the GDP representation of distillation columns is used to model the separation network. The reliability and efficiency of the proposed optimization method are demonstrated on two case studies, i.e., one cyclohexane oxidation process and one benzene chlorination process. The flowsheet structure and process-unit operating conditions are simultaneously optimized to minimize the total annual cost of the processes.

Keywords: reaction-separation process design; process optimization; generalized disjunctive programming; cyclohexane oxidation; benzene chlorination

1. INTRODUCTION

There is no doubt that systematic process design has been playing an important role in the development of the chemical society. Over the past decades, various work on process design and process synthesis has been carried out.^{1,2} As chemical engineers, it is common practice to decompose the overall design problem into sub-problems such as reactor network design and separation network synthesis.³⁻⁵ This is because the simultaneous design of reaction-separation processes leads to combinatorial explosion. In combination with the strong nonlinearities embedded in process and thermodynamic models, the resulting mathematical optimization is a challenging task. However, due to the strong and complex interactions between reaction and separation systems the change of any condition in any unit can significantly affect the performance of the entire chemical process.⁶ Thus, the development of reliable process design approaches with general applicability for reaction-separation processes is highly desirable.

Almost all chemical production processes begin with reactions. The existing methods for reactor network design can be mainly classified into heuristics, geometric attainable region, and superstructure-based optimization. Based on the long-term experience of chemical engineers and researchers, heuristic methods are usually applied for simple and well-understood reaction systems.⁷ Due to its sequential nature, the applicability of this method for complex systems is limited by the managements of interactions among different design levels. Attainable region concept which graphically represents the maximum achievable product composition can be directly used to generate the optimal reactor design for given reaction kinetics.⁸⁻¹³ But it is hard to apply this method to problems with more than three dimensions and multi-recycles. With the rapid development of efficient optimization algorithms and solvers, the superstructure-based optimization approach becomes attractive. In general, a superstructure containing possible

reactor configurations is predefined and the structure is formulated as (mixed-integer) nonlinear programming problems.¹⁴⁻²⁰ Furthermore, optimization techniques can also be coupled with the attainable region concept to enable the construction of multi-dimensional attainable regions.^{13,20}

Unlike the multidirectional developments of reactor network design, the research of optimal design of complex separation systems primarily focused on optimization-based approaches. Short-cut methods such as Underwood method,²¹ boundary value method,²² or rectification body²³ method are generally used at the preliminary design stage to provide a rough and quick estimation. Moreover, simulation-based optimization approaches have been applied to design complex distillation systems.^{24,25} Concerning the rigorous modeling of distillation columns where both discrete and continuous variables are involved, there are two major formulations: mixed-integer nonlinear programming (MINLP)^{26,27} and generalized disjunctive programming (GDP).³⁰⁻³³ In the MINLP representation, the number of equilibrium trays are determined by the variable locations of feed tray, reflux, and boil-up. To improve its robustness and applicability, the reformulation as a purely continuous optimization problem and external thermodynamic function has been introduced.^{28,29} In the GDP approach trays are modeled as permanent and conditional ones (see Section 3.2 for more information). Barttfeld et al.³³ compared the solution properties of those two approaches (i.e., MINLP and GDP). They indicated that the use of logic-based disjunctions and propositions in the GDP model greatly improves the modeling robustness and the computational efficiency. Importantly, on the basis of the state equipment network (SEN) and state tank network (STN) representations the GDP methodology can be easily extended to the synthesis of complex column configurations.^{31,32}

For considering the strong interactions between reaction and separation systems, great progresses have also been made for the determination of optimal process configuration. Kokossis

and Floudas formulated the synthesis of isothermal reactor-separator-recycle systems as MINLP.³⁴ Hentschel et al.⁶ coupled the innovative elementary process function concept with process-wide optimization technique to obtain the best process parameters. Additionally, Linke and Kokossis used two stochastic optimization technologies to synthesize global optimal configurations of reaction-separation systems.³⁵ However, in these contributions short-cut distillation models are used to reduce the design complexity. The usage of short-cut models can result in large inaccuracy since these models are based on ideal system assumptions which are often invalid in most industrial cases. Moreover, detailed design information such as equipment sizes and costs cannot be offered using short-cut models. To overcome these limitations, simulation-based optimization has been proposed.³⁶⁻³⁹ On the one hand, the coupling of stochastic algorithms and rigorous process simulations were implemented.³⁶ However, the reliability of this method is limited when the number of design variables increases. On the other hand, surrogate models can be built from the regression of simulation-based data.³⁷⁻³⁹ Later, the original process models are replaced by the surrogate models, through which the complexity of process optimization is significantly reduced. Nevertheless, without the usage of physical simplifications these models often involve a bumpy and complex functional form which is undesired for algebraic optimizations.⁴⁰ Additionally, the accuracy of surrogate models is usually limited by the insufficient sampled data. Recker et al.⁴¹ proposed an optimization-based framework for integrated reaction-separation process design where multiple connections between reaction and separation systems are considered. Process alternatives are enumerated using heuristics and prescreened using shortcut models. Promising candidates are further optimized using rigorous process models. This incremental refinement allows for a reduction in the number of structural decision variables and thus increases the numerical robustness. However, the

optimal process may have been discarded during the initial prescreening stage due to the incomplete enumeration and/or the deviation of the shortcut models.

In conclusion, rigorous and simultaneous reaction-separation process design is necessary for achieving efficient chemical processes. Conventional methods cannot efficiently address the problem because of the large and complex design space. For the optimization-based process design either simplified process models or knowledge-based heuristic methods have been applied to reduce the computational complexity. Recently the GDP models have been proven to be very efficient for the modeling of discrete and continuous optimization problems.⁴² These considerations motivate us to develop GDP models for the rigorous and simultaneous design of reaction and separation processes. Note that only the traditional ‘reaction followed by separation’ structure is considered in this work.

The paper is organized as follows. First, the design problem is stated. Afterwards, two GDP model-based reactor superstructures are proposed and the existing GDP model for the design of separation systems is briefly outlined. Finally, the performance of the proposed design approach is demonstrated on two industrial examples.

2. PROBLEM STATEMENT

For a given reaction system with known kinetics and thermodynamic data, the objective is to generate an economically optimal process under a specified product production rate. In the process, a reactor network is followed by a sequence of distillation columns that is used to recover unconverted reactants and purify the products to certain purities. The flowsheet structure including the types of reactor, interconnection between reactors, and separation sequences, the unit specifications such as the reactor and heat exchanger sizes, number of trays, as well as the

process operating conditions (e.g., reflux ratios) are the variables to be optimized to minimize the total annual cost (TAC) of the process.

In the proposed design problem several assumptions are made:

- Only ideal reactors: continuous stirred tank reactor (CSTR) and plug flow reactor (PFR) are considered in the reactor network. External utilities are used to maintain isothermal operation inside the reactor. Constant liquid densities are also assumed.
- Simple distillation columns with one feed and two outlet streams are used. Total condenser and partial reboiler are considered. Besides, the cooling and heating requirements are provided only by external utilities (i.e., cooling water and steam) and no heat integration is used. All the distillation columns are operated at 1 atm. Thus, the vapor phase is treated as an ideal gas.

Despite the above model simplifications, the proposed design method is considered rigorous from the perspective that it enables the simultaneous optimization of structural and operational variables for all possible process configurations.

3. MODEL DESCRIPTION

In general, the overall superstructure consists of two networks: the reactor network and the separation network.

3.1. Reactor Network

The academic and industrial research on reactor network design is attractive since the reactor is regarded as the heart of an overall chemical process. Extensive reviews of systematic approaches for reactor network design can be found in the literature.^{17,41} Previously, research focused on the manipulation and adjustment of mixing patterns within the reactor.¹⁸ It is well known that PFR is assumed without back-mixing along the reactor horizon and CSTR assumes

perfect back-mixing inside the tank. A real-world reactor can be always approximated by a cascade of CSTRs. Later on, attention has been paid to the determination of optimal structures from a given set of reactors.¹⁴⁻¹⁷ For considering the two distinct research interests, we propose two different reactor superstructures based on GDP models.

Figure 1 shows the first reactor superstructure with N consecutive reactor units. Each unit consists of two options: one isothermal CSTR and bypass. A Boolean variable Y_n is assigned to the n -th reactor unit. When Y_n is true, the associated CSTR exists and the corresponding mass and energy balance equations are then activated as written in eq 1. Otherwise, the second option “bypass” is activated which leads to a non-existent reactor. In this case, the states including temperature, enthalpy, and molar flowrates of the inlet stream are forced to be equal to those of the outlet streams. The disjunctive n -th reactor unit is formulated as follows:

$$\left[\begin{array}{c} Y_n \\ \dot{F}_{n,out}^i = f_{CSTR}(\dot{F}_{n-1,out}^i, T_{n,out}, P_n, \tau_n) \\ h_{n,out}^i = h(T_{n,out}) \\ \dot{Q}_n = \sum_i (\dot{F}_{n,out}^i \cdot h_{n,out}^i - \dot{F}_{n-1,out}^i \cdot h_{n-1,out}^i) \\ \tau_n > 0 \end{array} \right] \vee \left[\begin{array}{c} \neg Y_n \\ \dot{F}_{n,out}^i = \dot{F}_{n-1,out}^i \\ h_{n,out}^i = h_{n-1,out}^i \\ \dot{Q}_n = 0 \\ \tau_n = 0 \end{array} \right] \quad \begin{array}{l} n = 1, \dots, N \\ i = 1, \dots, N_c \end{array} \quad (1)$$

where the superscript i represents the component index and N_c is the total number of components. n denotes the n -th disjunctive reactor unit. Note that the outlet stream of the $(n-1)$ -th reactor disjunction is the inlet stream of the n -th reactor disjunction. When n is 1, $\dot{F}_{0,out}^i$ and $h_{0,out}^i$, normally given, stand for the molar flowrates and enthalpy of the initial inlet stream, respectively. \dot{F} , h , T , P , and τ are molar flowrates, enthalpy, temperature, pressure, and residence time, respectively. T , P , and τ are usually considered as reactor design variables. f_{CSTR} represents the function to determine the outlet flowrates (also compositions) from the inlet flowrates, temperature, pressure, and residence time of the reactor. External utilities are used to maintain isothermal operations in the reactor. If the reaction takes place (i.e., when Y_n is true),

the total enthalpy of the reactor inlet stream is different from that of the outlet stream due to the different temperatures and mixture compositions. This enthalpy difference indicates exactly the heat (\dot{Q}_n) we need to supply or to remove.

The following logic constraint is added to ensure that the existence of CSTRs can only be activated from the left to the right:

$$Y_n \Rightarrow Y_{n-1}, \quad n = 2, \dots, N \quad (2)$$

It is worth noting that when Y_1 is true and all the other Boolean variables are false, the resulting reactor network is one CSTR. When the maximum number of reactor disjunctions, N , is set to a very large number and all the Boolean variables are true, the resulting reactor network approximates a PFR. Lastly, when some of the Boolean variables are true and the rests are false, it corresponds to an intermediate state between CSTR and PFR which approximates the real-world non-ideal reactor.

The other reactor superstructure we proposed involves M PFRs and N CSTRs in series, parallel, series followed by parallel, and parallel followed by series (see Figure 2). As shown, this inverted triangular superstructure has maximal $(M+N)$ rows and $(M+N)$ columns. It contains $(M + N + 1) \times (M + N)/2$ reactor units. The modeling logic can be described as follows: Assume that all the M PFRs and N CSTRs are needed for a reaction. Considering the first extreme scenario where M PFRs and N CSTRs are in parallel, it corresponds to $(M+N)$ rows and 1 column. Then, considering the second scenario where only one reactor exists in the first column, the second column can have maximal $(M+N-1)$ reactors in parallel. In the same manner, the last extreme scenario where M PFRs and N CSTRs are in series corresponds to 1 row and $(M+N)$ columns. Thus, it is found that a triangular superstructure, like Figure 2, is suitable to incorporate all the possible reactor alternatives involving M PFRs and N CSTRs. For each

reactor unit, there are three conditional options: PFR, CSTR, and bypass. The existences of these options are controlled by the Boolean variables: $Y_{s,k}^{CSTR}$, $Y_{s,k}^{PFR}$, $Y_{s,k}^{bypass}$. If $Y_{s,k}^{CSTR}$ is true, the associated algebraic equations describing mass and energy balances of CSTR are enforced. If $Y_{s,k}^{PFR}$ is true, the mass and energy balance equations of PFR are activated. These balance equations can be solved by integrating differential equations. For simple reactions (e.g., first-order reactions investigated in this work), analytical solutions are obtained. Otherwise, the “bypass” option will be selected which makes the states (i.e., flowrates, enthalpy, and temperature) of the inlet stream equal to those of the outlet stream. As a result, the reactor disjunction is formulated as follows:

$$\begin{aligned}
 & \left[\begin{array}{c} Y_{s,k}^{CSTR} \\ \dot{F}_{s,k,out}^i = f_{CSTR}(\dot{F}_{s,k,in}^i, T_{s,k,out}, P_{s,k}, \tau_{s,k}) \\ h_{s,k,in}^i = h(T_{s,k,in}) \\ h_{s,k,out}^i = h(T_{s,k,out}) \\ \dot{Q}_{s,k} = \sum_i (\dot{F}_{s,k,out}^i \cdot h_{s,k,out}^i - \dot{F}_{s,k,in}^i \cdot h_{s,k,in}^i) \\ \tau_{s,k} > 0 \end{array} \right] \vee \left[\begin{array}{c} Y_{s,k}^{PFR} \\ \dot{F}_{s,k,out}^i = f_{PFR}(\dot{F}_{s,k,in}^i, T_{s,k,out}, P_{s,k}, \tau_{s,k}) \\ h_{s,k,in}^i = h(T_{s,k,in}) \\ h_{s,k,out}^i = h(T_{s,k,out}) \\ \dot{Q}_{s,k} = \sum_i (\dot{F}_{s,k,out}^i \cdot h_{s,k,out}^i - \dot{F}_{s,k,in}^i \cdot h_{s,k,in}^i) \\ \tau_{s,k} > 0 \end{array} \right] \vee \\
 & \left[\begin{array}{c} Y_{s,k}^{bypass} \\ \dot{F}_{s,k,out}^i = \dot{F}_{s,k,in}^i \\ h_{s,k,out}^i = h_{s,k,in}^i \\ T_{s,k,out} = T_{s,k,in} \\ \dot{Q}_{s,k} = 0 \\ \tau_{s,k} = 0 \end{array} \right] \quad s, k = 1, \dots, (M + N) \quad (3)
 \end{aligned}$$

where the subscripts s and k represent the row number and column number, respectively (see Figure 2). Upon the size of the triangular superstructure, s and k must fulfill the following constraint:

$$s + k \leq M + N + 1, \quad s, k = 1, \dots, (M + N) \quad (4)$$

The connectivity equations for mass and energy flows can be represented as:

$$\sum_s \dot{F}_{s,k,in}^i - \sum_s \dot{F}_{s,k-1,out}^i = 0, \quad k = 2, \dots, (M + N) \quad (5)$$

$$\sum_s h_{s,k,in}^i \cdot \dot{F}_{s,k,in}^i - \sum_s h_{s,k-1,out}^i \cdot \dot{F}_{s,k-1,out}^i = 0, \quad k = 2, \dots, (M + N) \quad (6)$$

Additionally, logic equations are applied to avoid multiple solutions. Eq 7 is used to guarantee that only one option is selected for one reactor disjunction. Eq 8 and eq 9 ensure that the maximal number of PFRs and CSTRs are M and N , respectively. Finally, for every column, eq 10 forces the reactors to be activated from top to bottom only. Eq 11 is used to ensure the reactors are placed from left to right in the first row.

$$Y_{s,k}^{CSTR} \vee Y_{s,k}^{PFR} \vee Y_{s,k}^{bypass}, \quad s, k = 1, \dots, (M + N) \quad (7)$$

$$[Y_{1,1}^{PFR}, Y_{2,1}^{PFR}, \dots, Y_{M+N,1}^{PFR}, Y_{1,2}^{PFR}, \dots, Y_{1,M+N}^{PFR}] \text{ at most } M \text{ true} \quad (8)$$

$$[Y_{1,1}^{CSTR}, Y_{2,1}^{CSTR}, \dots, Y_{M+N,1}^{CSTR}, Y_{1,2}^{CSTR}, \dots, Y_{1,M+N}^{CSTR}] \text{ at most } N \text{ true} \quad (9)$$

$$Y_{s-1,k}^{bypass} \Rightarrow Y_{s,k}^{bypass}, \quad s = 2, \dots, (M + N), \quad k = 1, \dots, (M + N) \quad (10)$$

$$Y_{1,k-1}^{bypass} \Rightarrow Y_{1,k}^{bypass}, \quad k = 2, \dots, (M + N) \quad (11)$$

Comparing to the traditional MINLP representation,^{14,16,17} this GDP model is more systematic and easier to establish.

3.2. Separation Network

Two different modeling approaches, namely MINLP and GDP, have been employed for the rigorous modeling of single distillation columns. The GDP model for single-column design has been initially proposed by Yeomans and Grossmann.³⁰ The authors claimed that comparing to the MINLP model, the GDP model reduces redundant balance equations and thus leads to an improvement in the computational efficiency and robustness. Barttfeld et al.³³ proposed two column representations, fixed feed location and variable feed location, using the GDP formulation. Here, we only provide a brief overview on the first representation (see Figure 3), which is utilized in this work. The main idea is to divide the column trays into two categories:

permanent and conditional trays. As shown in Figure 3a, the permanent trays including the condenser, reboiler, and feed tray are modeled as equilibrium stages. All the MESH equations³¹ (i.e., mass balances, equilibrium equations, summation equations, and energy balances) are fulfilled in these trays. The trays between the permanent trays are conditional trays whose existences depend on the values of the associated Boolean variables. If the Boolean variable is true, the tray is modeled as an equilibrium tray. Otherwise, vapor and liquid streams directly pass the tray without mass and energy transfer, which means the tray does not exist. After optimization, the optimal column configuration will be obtained where the non-existent trays are automatically ignored, as plotted in Figure 3c.

In the GDP model³¹, the trays of the column ($m = 1, \dots, N_{FT}, \dots, N$) are numbered from bottom to top. Because there is the possibility of deleting or deactivating different conditional trays for the same total number of trays, it is possible to obtain multiple solutions with the same objective function value. To avoid this situation, the following logic constraints are employed to enforce the selected trays being activated above and below the feed tray.

$$Z_m \Rightarrow Z_{m-1}, m > N_{FT} \quad (12)$$

$$Z_m \Rightarrow Z_{m+1}, m < N_{FT} \quad (13)$$

where Z_m is the Boolean variable indicating the existence of the m -th tray and N_{FT} denotes the feed tray number.

As pointed out by Yeomans and Grossmann,³¹ the SEN representation is more suitable for the rigorous modeling of distillation sequences since it yields a less number of variables and equations compared to the STN representation. In our case studies, only zeotropic separation is considered. Thus, the superstructure is composed of $(N_c - 1)$ columns where N_c is the total number of components to be separated. For instance, the SEN representation for the separation of

3-component mixtures is shown in Figure 4. In this superstructure, each column has two different separation tasks. The decision-making on the selection of separation tasks in the column can be controlled by the specification of component purity and recovery. Specifically, the disjunctions are written as:

$$\vee \begin{bmatrix} Y_{c,t} \\ y_{c,t}^i \geq \xi_{c,t}^i \\ \gamma_{c,t}^i \geq \theta_{c,t}^i \end{bmatrix} \quad c = 1, \dots, (N_c - 1) \quad (14)$$

where t is the set of separation tasks that might occur in a certain column c . For separation task t , $\xi_{c,t}^i$ and $\theta_{c,t}^i$ represent the specifications of purity y^i and recovery γ^i on t -dependent key component i on the top or bottom of column c . Additionally, logic relationships are required to enforce the consistency of tasks in the columns. For separating 3-component zeotropic mixtures, the following constraints should be applied.

$$Y_{1,A/BC} \underline{\vee} Y_{1,AB/C} \quad (15)$$

$$Y_{1,A/BC} \Rightarrow Y_{2,B/C} \quad (16)$$

$$Y_{1,AB/C} \Rightarrow Y_{2,A/B} \quad (17)$$

Eq 15 ensures that only one separation task can be selected in the first column. Eq 16 and 17 guarantee the consistency of different tasks. For more information about the SEN representation based superstructure modeling of multicomponent distillation columns and separation sequences, please refer to ref 33, 43.

3.3. Cost Estimation

The objective of our rigorous design of reaction-separation processes is to minimize the process TAC that includes capital and operational costs (see eq 18). The capital costs C_a including costs for reactors, heat exchangers, and distillation columns are estimated based on the nonlinear models given in ref 6, 28. The operational cost C_{op} is directly calculated from the

consumption of cooling water and high-pressure steams. For the detailed calculation of C_a and C_{op} for each process unit, please refer to the Appendix and Supporting Information.

$$\min \quad TAC = C_a + C_{op} \quad (18)$$

4. CASE STUDY

The proposed design method is illustrated by two industrial examples. The optimization is implemented in GAMS 24.3.1 on a PC with an Intel(R) core(TM) i5-2400 CPU at 3.10GHz with 8 GB RAM running on the 64 bit Windows 7 Enterprise operating system. Firstly, the GDP models are reformulated into MINLP models by the Big-M approach through the GAMS solver JAMS 1.0. Then, the generated MINLP problem is solved by the standard branch-and-bound solver SBB and the NLP solver CONOPT 3.

4.1. Cyclohexane Oxidation Process

Cyclohexane oxidation is a very important process in the chemical industry for producing cyclohexanone and cyclohexanol (also known as ‘KA’ oil), which are used as intermediates in the manufacturing of Nylon-6 and Nylon-6, 6. The entire reaction network can be characterized by about 35 radical reactions with 20 components. Alagy et al.⁴⁴ proposed a simplified reaction scheme as shown in Scheme 1. Based on this scheme and a set of experimental kinetic data, Krzysdoforsk et al.⁴⁵ regressed the first-order reaction rate constants $k_1 - k_4$, as presented in Table S1 in the Supporting Information.

4.1.1. Superstructure Initialization

As shown in Figure 5, a superstructure consisting of 10 consecutive reactor disjunctions and two distillation columns is initialized where A, B, C, and D denote cyclohexane, cyclohexanol, cyclohexanone, and adipic acid, respectively and the mixture of B and C is the desired product. The involved parameters, specifications, and operating conditions are listed in Table S1

(Supporting Information). The number of activated reactors and the corresponding residence time are considered as design variables in the reactor network. The design variables in the separation network include the separation sequence, the number of trays, the position of feed trays, and reflux ratios of columns.

4.1.2. Results

The optimal process configuration is shown in Figure 6. Since the products (i.e., cyclohexanol and cyclohexanone) are much more reactive than the raw material cyclohexane, over-oxidation must be carefully avoided in the reaction. It is for this reason that one single PFR is not suitable because we need to have a certain degree of back-mixing in the reactor in order to reduce the product concentrations. On the other hand, if only one CSTR is applied, a large amount of cyclohexane has to be fed into the reactor to meet the specified product production rate and the single-pass conversion should be set to a relatively low value in order to reduce the production of the by-product adipic acid. Two independent CSTRs are obtained from our optimization, as shown in Figure 6. The residence time in the first reactor is larger than that in the second one. This is because in the beginning a long reaction time (i.e., large reactor) allows for an initial accumulation of the product. A relatively small residence time in the second reactor is favorable to hinder the over-oxidation. For the distillation, the direct separation sequence is identified which removes the lightest abundant component (cyclohexane) from the top of the first column. This finding agrees well with the classical separation guidelines.

The computational results are listed in Table 1. It is worth mentioning that due to the large number of infeasible or invalid combinations of binary variables (71 of 150 nodes), substantial CPU time is spent on the calculation of the NLP sub-problems.

The optimal solution yields a total annualized cost of 2.23×10^6 \$/year. Table 2 summarizes the optimized costs for each process unit. Moreover, the resulted design is compared with a reference design adopted from industrial processes, as shown in Table 3. For both designs, the production rate of the main product is fixed to 50 kmol/h. The industrial cyclohexane oxidation process uses 5 consecutive CSTRs with the same size. Additionally, the reaction conversion is limited to 4% and the selectivity is 80% – 85%.⁴⁵ Based on this information, the corresponding reactor outflows can be estimated. Since the data of the distillation columns in the industrial process is confidential and has not been published, the separation network is optimized using the rigorous tray-by-tray models based on the reactor outflows. Finally, the reference design for the cyclohexane oxidation process is obtained by combining the industrial reactor design and our optimized separation network. From Table 3, it can be seen that the process designed from our method is more economic than the reference design.

4.2. Benzene Chlorination Process

Benzene chlorination is one of the first industrialized processes for manufacturing organic chemicals. In this reaction, benzene is primarily converted to monochlorobenzene, and dichlorobenzene whose ratio depends on the reaction conditions. Monochlorobenzene is an important chemical intermediate for the production of phenol, aniline, and dichloro-diphenyl-trichloroethane (DDT). Dichlorobenzene can be used to produce larvicide and deodorant. In this case study, we consider monochlorobenzene as the desired product and dichlorobenzene treated as a byproduct. The reaction scheme is given in Scheme 2. In this example, the reactor selection and its residence time should be determined in the reactor network. In the separation network, the separation sequence, the number of trays, the position of feed tray, and the reflux ratio in each column are considered as design variables.

4.2.1. Superstructure Initialization

Figure 7 shows the superstructure for the benzene chlorination process with A, B, and C indicating benzene, monochlorobenzene, and dichlorobenzene, respectively. The second reactor superstructure proposed in this work (see Figure 2) is employed to design the reactor network. For considering the simplicity of the reaction, the simplest structure (with $M = 1$ and $N = 1$) is chosen to reduce the computational complexity. The process operating conditions as well as the important parameters and specifications are listed in Table S4 (Supporting Information).

4.2.2. Results

The optimal process configuration can be found in Figure 8. Since the reaction rate constant of the main reaction is much larger than that of the side reaction, a high benzene concentration is preferable for the production of monochlorobenzene. To maintain the high concentration of benzene, back-mixing effects should be minimized. This explains why only one single PFR is obtained from the optimization.

The computational results are presented in Table 4. By comparing with Table 1, we find even though the searched NLP nodes are more than that in the first case study, the CPU time is much less. This is mainly due to the different non-linearity levels of the two case studies, which can be indicated by the different number of nonlinear matrix entries (7290 versus 2405). In addition, the size of the NLP problem in the first example is also bigger than that in this one, which is reflected by the different number of equations and variables.

The optimal objective function (TAC) is 6.24×10^5 \$/year. Table 5 shows a summary of the final capital investment and operational cost for the main process units. Similar to the first case study, a reference design for the benzene chlorination process is also obtained based on the work from Shah and Kokossis⁴⁶ where the authors applied engineering heuristics and shortcut models

to design the process. From the comparison in Table 6, the process designed in this work is more economic than the reference design, which suggests the importance of applying rigorous distillation models to design reaction-separation processes.

For both case studies, the reference design uses a relatively low reaction conversion to ensure a high selectivity. This leads to a larger amount of unconverted reactants flowing into the distillation section where they are separated and recovered. It explains why the cost of the reactors is low but the cost for the distillation columns is much higher than that of our optimal design.

It is worth mentioning that in order to increase the probability of finding high-quality solutions, we used many different initial guesses to solve the problems. Even though different results were obtained, the flowsheet structures are the same and the objective function values are quite close. Additionally, the global optimization solver BARON⁴⁷ was also employed in this work. After a long computational time (about 24 hours), the upper bounds found by BARON are very close to our final results. These facts all suggest that the obtained optimal solutions are trustable.

5. CONCLUSION

This paper presents a new optimization-based approach for the rigorous design of reaction-separation processes. Starting from a predefined process superstructure, the structural decision variables and process operating variables are simultaneously optimized. The proposed method has been applied to a cyclohexane oxidation process and a benzene chlorination process. The effectiveness of the method is demonstrated through the comparison with reference designs for both case studies.

It is important to mention that due to the nonconvex models, global optimality cannot be guaranteed by the solver we used. Obviously, the use of global MINLP solvers such as BARON will increase the reliability and applicability of the results. However, in that case, the solvability and computational cost are likely to become the limiting factors. In general, more advanced model reformulation strategy or mathematical algorithms should be developed in order to improve the performance of the proposed method. In our current work, several different initial guesses are simply used to increase the possibility of finding high-quality optimal solutions.

Appendix. Sizing and Cost Models

The capital investments involved in this work include the purchase and installation costs for the reactors, heat exchangers, and distillation columns.

$$C_a = C_{rt} + C_{he} + C_{dc} \quad (\text{A.1})$$

where the subscripts *rt*, *he*, and *dc* represent the reactor, heat exchanger, and distillation column, respectively.

The operational cost C_{op} depends on the consumption of cooling water and steam.

$$C_{op} = C_{steam} \cdot m_{steam} + C_{water} \cdot m_{water} \quad (\text{A.2})$$

where C_{steam} and C_{water} are the mass-based unit prices of steam and cooling water, respectively. m_{steam} and m_{water} represent the total mass flowrates of steam and water, respectively. The steam is used in the heat exchanger and reboiler. The cooling water is used in the reactor and condenser. All the employed cost estimation equations are taken from ref 6, 28.

a) Reactor

The capital cost of the n -th reactor is related to its characteristic dimensions: diameter D_n and length L_n . The reactor volume V_n is calculated by multiplying the residence time τ_n with the

volumetric flowrate of the reactor inlet stream \dot{V}_n which equals to \dot{V}_0 under the constant liquid density assumption. Assuming that the reactor is a vessel whose length is four times of its diameter,⁶ the base cost (BC_n) of the n -th reactor and the total cost of all the reactors (C_{rt}) are calculated as:

$$V_n = \dot{V}_0 \cdot \tau_n \quad (\text{A.3})$$

$$D_n = \sqrt[3]{\frac{V_n}{\pi}} \quad (\text{A.4})$$

$$L_n = 4 \cdot D_n \quad (\text{A.5})$$

$$BC_n = 1000 \cdot \left(\frac{D_n}{0.9144}\right)^{1.05} \cdot \left(\frac{L_n}{1.2192}\right)^{0.81} \quad (\text{A.6})$$

$$C_{rt} = \sum_{n=1}^N \frac{0.75 \times 585 \times 4.23 \times BC_n}{115} \quad (\text{A.7})$$

b) Heat Exchanger

In the second case study, the capital cost of the heat exchanger depends on the heat transfer area A_{he} , as shown below:

$$C_{he} = 3100 \cdot A_{he}^{0.65} \quad (\text{A.8})$$

The heat transfer area can be obtained from:

$$A_{he} = \left| \frac{\dot{Q}_{he}}{U \cdot \Delta T_{he}} \right| \quad (\text{A.9})$$

Here, U is the heat transfer coefficient; \dot{Q}_{he} and ΔT_{he} are the required heat duty and the logarithmic mean temperature difference (LMTD) of the heat exchanger, respectively.

c) Distillation Column

The employed cost model for distillation columns is from Kossack et al.²⁸ The capital investment for each distillation column is comprised of the cost of column shell C_{shell} , column internals $C_{internal}$, reboiler C_{rb} , and condenser C_{cd} which are evaluated by:

$$C_{dc} = C_{shell} + C_{internal} + C_{rb} + C_{cd} \quad (\text{A.10})$$

$$C_{shell} = 4100 \cdot D_{dc} \cdot H_{dc} \quad (A.11)$$

$$C_{internal} = 1800 \cdot D_{dc} \cdot \Delta H \cdot NT \quad (A.12)$$

where D_{dc} , H_{dc} , and NT denote column diameter, column height, and the number of trays. ΔH is the height of one tray which is specified as 0.5 m in this work. Thus the column height H_{dc} is proportional to the number of trays:

$$H_{dc} = \Delta H \cdot NT + 4 \quad (A.13)$$

The column diameter D_{dc} is assumed to be equal to the diameter of the tray at the bottom of the column.

$$D_{dc} = D_{bottom} = \sqrt{\frac{4 \cdot \dot{V}_b}{2 \cdot \pi} \sqrt{\frac{R \cdot T_b \cdot (\sum y^i \cdot M^i)}{P}}} \quad (A.14)$$

where \dot{V}_b , T_b , R , and P are the vapor flowrate at bottom, the vapor temperature at bottom, the universal gas constant (8.3145 J/(mol·K)) and the column pressure (1 atm). y^i and M^i represent the vapor molar fraction of species i at the bottom of the column and molecular weight of species i , respectively. The capital cost of reboiler and condenser is calculated as follows.

$$C_{rb} + C_{cd} = 3100 \cdot (A_{rb} + A_{cd})^{0.65} \quad (A.15)$$

Here, A_{rb} and A_{cd} are the required heat exchanger areas of the reboiler and condenser, respectively. The areas are related to the amount of heat to be provided or removed.

$$A_{rb} = \frac{\dot{Q}_{rb}}{U \cdot \Delta T_{rb}} \quad (A.16)$$

$$A_{cd} = \frac{\dot{Q}_{cd}}{U \cdot \Delta T_{cd}} \quad (A.17)$$

where \dot{Q}_{rb} and \dot{Q}_{cd} are the heat duties of the reboiler and condenser, respectively. ΔT_{rb} and ΔT_{cd} are the LMTD of the reboiler and condenser, respectively.

SUPPORTING INFORMATION

The supporting information file provides the component physical properties and thermodynamic parameters as well as the auxiliary equations for calculating the sizes and costs.

ABBREVIATIONS

CSTR = continuous stirred tank reactor

DDT = dichloro-diphenyl-trichloroethane

GDP = generalized disjunctive programming

MINLP = mixed-integer nonlinear programming

NLP = nonlinear programming

PFR = plug flow reactor

SEN = state equipment network

STN = state tank network

TAC = total annual cost

REFERENCES

- (1) Chen, Q.; Grossmann, I. E. Recent developments and challenges in optimization-based process synthesis. *Annu. Rev. Chem. Biomol. Eng.* **2017**, in press.
- (2) Tula, A. K.; Eden, M. R.; Gani, R. Process synthesis, design and analysis using a process-group contribution method. *Comput. Chem. Eng.* **2015**, *81*, 245-259.
- (3) Daichendt, M. M.; Grossmann, I. E. Integration of hierarchical decomposition and mathematical programming for the synthesis of process flowsheets. *Comput. Chem. Eng.* **1998**, *22* (1), 147-175.
- (4) Omtveit, T.; Wah, P. E.; Lien, K. M. Decomposed algorithmic synthesis of reactor-separation-recycle systems. *Comput. Chem. Eng.* **1994**, *18* (11), 1115-1124.
- (5) Kravanja, Z.; Grossmann, I. E. Multilevel-hierarchical MINLP synthesis of process flowsheets. *Comput. Chem. Eng.* **1997**, *21*, S421-S426.
- (6) Hentschel, B.; Peschel, A.; Freund, H.; Sundmacher, K. Simultaneous design of the optimal reaction and process concept for multiphase systems. *Chem. Eng. Sci.* **2014**, *115*, 69-87.
- (7) Douglas, J. M. *Conceptual Design of Chemical Processes*; McGraw-Hill: New York, 1988.
- (8) Hildebrandt, D.; Glasser, D. The attainable region and optimal reactor structures. *Chem. Eng. Sci.* **1990**, *45* (8), 2161-2168.
- (9) Hildebrandt, D.; Glasser, D.; Crowe, C. M. Geometry of the attainable region generated by reaction and mixing: with and without constraints. *Ind. Eng. Chem. Res.* **1990**, *29* (1), 49-58.
- (10) Feinberg, M.; Hildebrandt, D. Optimal reactor design from a geometric viewpoint—I. Universal properties of the attainable region. *Chem. Eng. Sci.* **1997**, *52* (10), 1637-1665.
- (11) Feinberg, M. Optimal reactor design from a geometric viewpoint. Part II. Critical sidestream reactors. *Chem. Eng. Sci.* **2000**, *55* (13), 2455-2479.
- (12) Feinberg, M. Optimal reactor design from a geometric viewpoint — III. Critical CFSTRs. *Chem. Eng. Sci.* **2000**, *55* (17), 3553-3565.

- (13) Pahor, B.; Irsic, N.; Kravanja, Z. MINLP synthesis and modified attainable region analysis of reactor networks in overall process schemes using more compact reactor superstructure. *Comput. Chem. Eng.* **2000**, *24* (2), 1403-1408.
- (14) Kokossis, A. C.; Floudas, C. A. Optimization of complex reactor networks—I. Isothermal operation. *Chem. Eng. Sci.* **1990**, *45* (3), 595-614.
- (15) Kokossis, A. C.; Floudas, C. A. Optimization of complex reactor networks—II. Nonisothermal operation. *Chem. Eng. Sci.* **1994**, *49* (7), 1037-1051.
- (16) Pahor, B.; Kravanja, Z.; Bedenik, N. I. Synthesis of reactor networks in overall process flowsheets within the multilevel MINLP approach. *Comput. Chem. Eng.* **2001**, *25* (4), 765-774.
- (17) Esposito, W. R.; Floudas, C. A. Deterministic global optimization in isothermal reactor network synthesis. *J. Global Optim.* **2002**, *22* (1), 59-95.
- (18) Achenie, L. E. K.; Biegler, L. T. Algorithmic synthesis of chemical reactor networks using mathematical programming. *Ind. Eng. Chem. Res.* **1986**, *25* (4), 621-627.
- (19) Achenie, L. E. K.; Biegler, L. T. A superstructure based approach to chemical reactor network synthesis. *Comput. Chem. Eng.* **1990**, *14* (1), 23-40.
- (20) Lakshmanan, A.; Biegler, L. T. Synthesis of optimal chemical reactor networks. *Ind. Eng. Chem. Res.* **1996**, *35* (4), 1344-1353.
- (21) Underwood, A. J. V. Fractional distillation of multicomponent mixtures. *Ind. Eng. Chem. Res.* **1949**, *41* (12), 2844-2849.
- (22) Levy, S. G.; Van Dongen, D. B.; Doherty, M. F. Design and synthesis of homogeneous azeotropic distillations. 2. Minimum reflux calculations for nonideal and azeotropic columns. *Ind. Eng. Chem. Res.* **1985**, *24* (4), 463-474.
- (23) Bausa, J.; Watzdorf, R. v.; Marquardt, W. Shortcut methods for nonideal multicomponent distillation: I. Simple columns. *AIChE J.* **1998**, *44* (10), 2181-2198.
- (24) Quirante, N.; Javaloyes, J.; Caballero, J. A. Rigorous design of distillation columns using surrogate models based on Kriging interpolation. *AIChE J.* **2015**, *61* (7), 2169-2187.

- (25) Caballero, J. A. Logic hybrid simulation-optimization algorithm for distillation design. *Comput. Chem. Eng.* **2015**, *72*, 284-299.
- (26) Viswanathan, J.; Grossmann, I. E. Optimal feed locations and number of trays for distillation columns with multiple feeds. *Ind. Eng. Chem. Res.* **1993**, *32* (11), 2942-2949.
- (27) Zou, X.; Cui, Y. H.; Dong, H. G.; Wang, J.; Grossmann, I. E. Optimal design of complex distillation system for multicomponent zeotropic separations. *Chem. Eng. Sci.* **2012**, *75*, 133-143.
- (28) Kossack, S.; Kraemer, K.; Marquardt, W. Efficient optimization-based design of distillation columns for homogeneous azeotropic mixtures. *Ind. Eng. Chem. Res.* **2006**, *45* (25), 8492-8502.
- (29) Skiborowski, M.; Harwardt, A.; Marquardt, W. Efficient optimization-based design for the separation of heterogeneous azeotropic mixtures. *Comput. Chem. Eng.* **2015**, *72*, 34-51.
- (30) Yeomans, H.; Grossmann, I. E. Optimal design of complex distillation columns using rigorous tray-by-tray disjunctive programming models. *Ind. Eng. Chem. Res.* **2000**, *39* (11), 4326-4335.
- (31) Yeomans, H.; Grossmann, I. E. Disjunctive programming models for the optimal design of distillation columns and separation sequences. *Ind. Eng. Chem. Res.* **2000**, *39* (6), 1637-1648.
- (32) Barttfeld, M.; Aguirre, P. A.; Grossmann, I. E. A decomposition method for synthesizing complex column configurations using tray-by-tray GDP models. *Comput. Chem. Eng.* **2004**, *28* (11), 2165-2188.
- (33) Barttfeld, M.; Aguirre, P. A.; Grossmann, I. E. Alternative representations and formulations for the economic optimization of multicomponent distillation columns. *Comput. Chem. Eng.* **2003**, *27* (3), 363-383.
- (34) Kokossis, A. C.; Floudas, C. A. Synthesis of isothermal reactor-separator-recycle systems. *Chem. Eng. Sci.* **1991**, *46* (5), 1361-1383.
- (35) Linke, P.; Kokossis, A. On the robust application of stochastic optimisation technology for the synthesis of reaction/separation systems. *Comput. Chem. Eng.* **2003**, *27* (5), 733-758.

- (36) Gross, B.; Roosen, P. Total process optimization in chemical engineering with evolutionary algorithms. *Comput. Chem. Eng.* **1998**, *22*, S229-S236.
- (37) Caballero, J. A.; Odjo, A.; Grossmann, I. E. Flowsheet optimization with complex cost and size functions using process simulators. *AIChE J.* **2007**, *53* (9), 2351-2366.
- (38) Caballero, J. A.; Grossmann, I. E. An algorithm for the use of surrogate models in modular flowsheet optimization. *AIChE J.* **2008**, *54* (10), 2633-2650.
- (39) Henao, C. A.; Maravelias, C. T. Surrogate-based superstructure optimization framework. *AIChE J.* **2011**, *57* (5), 1216-1232.
- (40) Cozad, A.; Sahinidis, N. V.; Miller, D. C. Learning surrogate models for simulation-based optimization. *AIChE J.* **2014**, *60* (6), 2211-2227.
- (41) Recker, S.; Skiborowski, M.; Redepenning, C.; Marquardt, W. A unifying framework for optimization-based design of integrated reaction–separation processes. *Comput. Chem. Eng.* **2015**, *81*, 260-271.
- (42) Grossmann, I. E.; Ruiz, J. P. Generalized disjunctive programming: A framework for formulation and alternative algorithms for MINLP optimization. In *Mixed Integer Nonlinear Programming*, Lee, J.; Leyffer, S., Eds. Springer New York: New York, NY, 2012.
- (43) Grossmann, I. E.; Aguirre, P. A.; Barttfeld, M. Optimal synthesis of complex distillation columns using rigorous models. *Comput. Chem. Eng.* **2005**, *29* (6), 1203-1215.
- (44) Alagy, J.; Trambouze, P.; Van Landeghem, H. Designing a cyclohexane oxidation reactor. *Ind. Eng. Chem. Res.* **1974**, *13* (4), 317-323.
- (45) Krzysztoforski, A.; Wojcik, Z.; Pohorecki, R.; Baldyga, J. Industrial contribution to the reaction engineering of cyclohexane oxidation. *Ind. Eng. Chem. Res.* **1986**, *25* (4), 894-898.
- (46) Shah, P.B.; Kokossis A. Design targets of separator and reactor-separator systems using conceptual programming. *Comput. Chem. Eng.* **1997**, *21*, S1013-1018.
- (47) Tawarmalani, M.; Sahinidis, N. V. A polyhedral branch-and-cut approach to global optimization. *Math. Program.* **2005**, *103* (2), 225-249.

Figure 1. Reactor superstructure with N reactor units

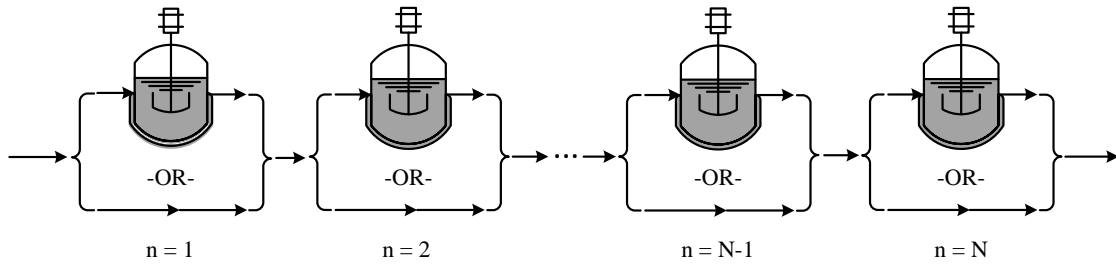


Figure 2. Reactor superstructure with multiple PFRs and CSTRs

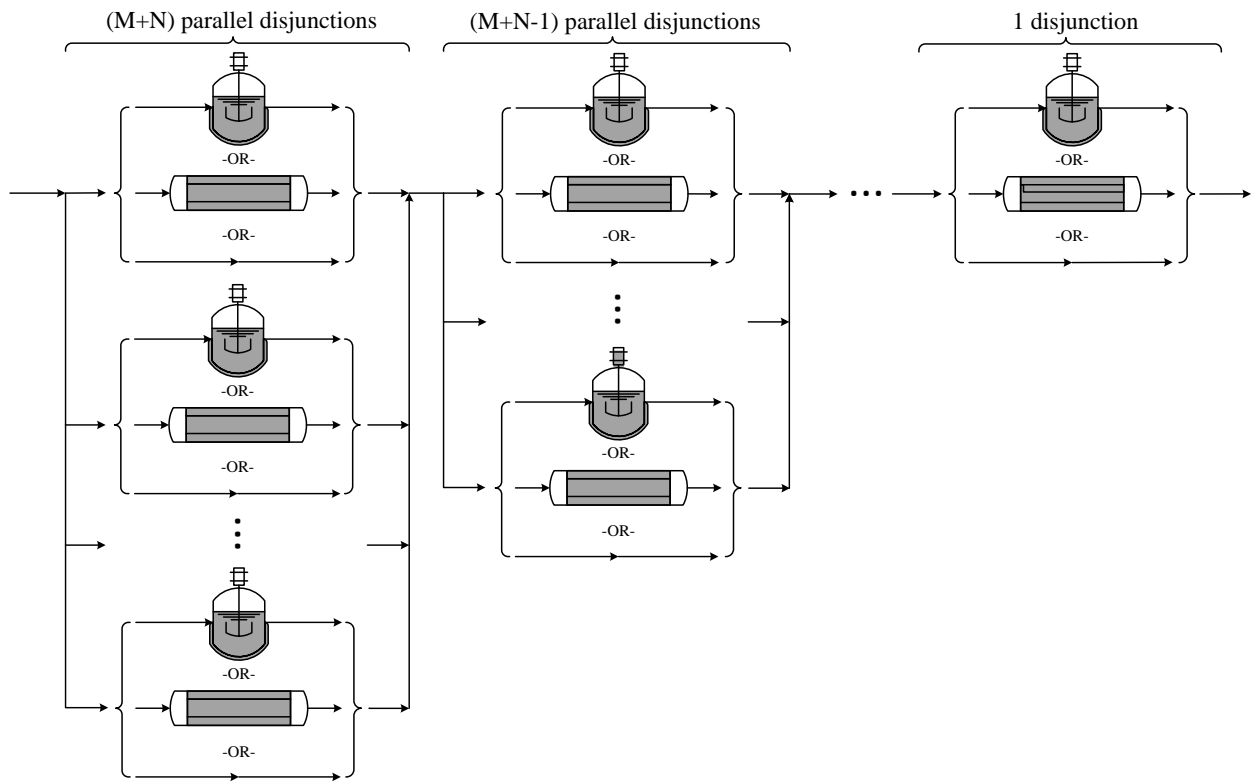


Figure 3. GDP representation of distillation columns

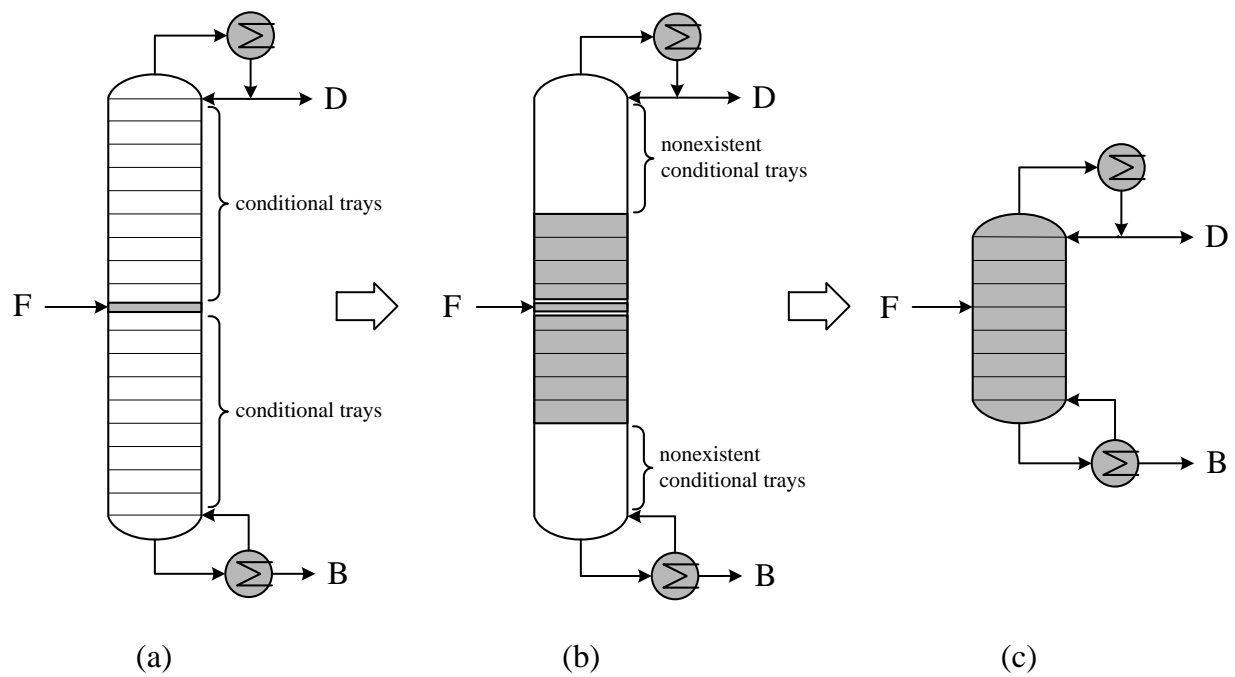
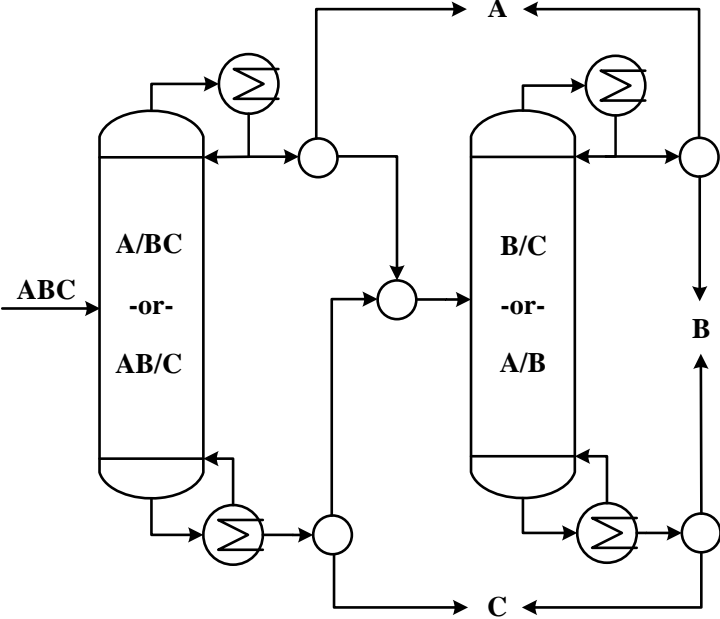


Figure 4. SEN representation based superstructure for 3-component distillation systems (A, B, and C are in order of decreasing relative volatility)



Scheme 1. Simplified Reaction Scheme for Cyclohexane Oxidation

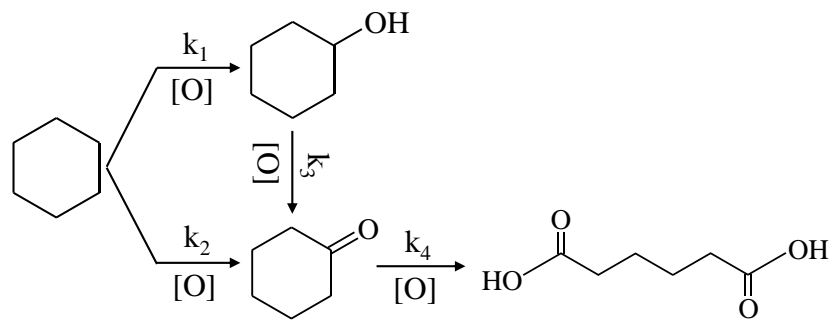


Figure 5. Initial superstructure for the cyclohexane oxidation process

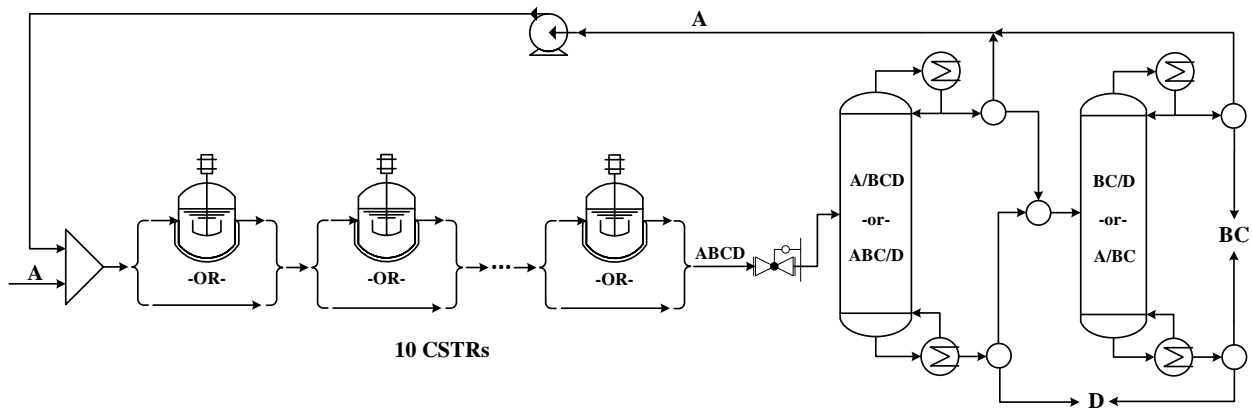


Figure 6. Optimal process configuration for the first case study (flowrate in kmol/h)

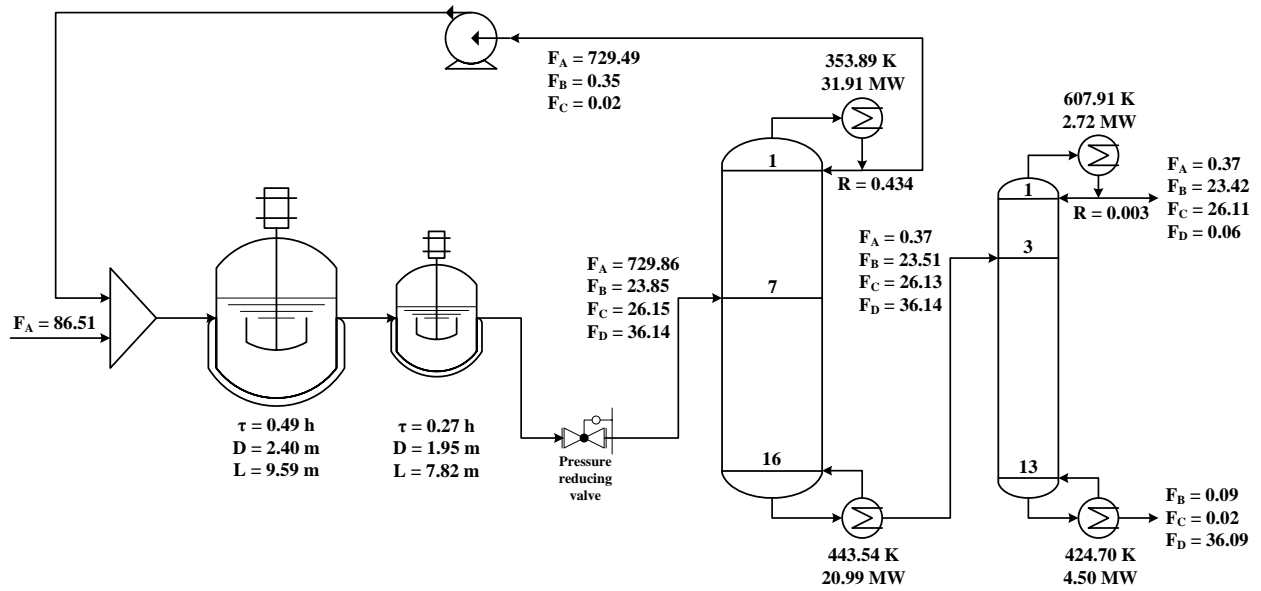


Table 1. Computational Results for the Cyclohexane Oxidation Case Study

Optimal TAC (\$/year)	2.23×10^6
TAC in the first relaxed NLP (\$/year)	4.12×10^5
Number of equations	4046
Number of discrete variables	91
Number of variables	3106
Number of nonlinear matrix entries	7290
Code length	28268
Searched SBB nodes	150
Infeasible nodes	71
CPU time (s)	377

Table 2. Economic Optimization Results for the Cyclohexane Oxidation Case Study

	Capital Investment (10 ⁵ \$/year)	Operational Cost (10 ⁵ \$/year)
1 st Reactor	2.36	0.81
2 nd Reactor	1.61	0.53
1 st Distillation column	3.40	9.29
2 nd Distillation column	1.17	3.11

Table 3. Comparison between Our Design Results and the Reference Design for the Cyclohexane Oxidation Case Study

	Reference Design	Our Design
Reactor network	5 CSTRs	2 CSTRs
Input flowrate (kmol/h)	1250	816
Reaction conversion	4.7%	10.6%
Reaction selectivity	85%	58%
Separation sequence	Direct separation	Direct separation
Feed location in the 1 st column	9	7
Number of trays in the 1 st column	18	16
Reflux ratio of the 1 st column	0.53	0.43
Feed location in the 2 nd column	11	3
Number of trays in the 2 nd column	20	13
Reflux ratio of the 2 nd column	0.003	0.003
TAC (\$/year)	2.86×10^6	2.23×10^6
Process profit (million \$/year)*	75.9	115.4

*Process profit = revenues of KA oil and adipic acid – cost of cyclohexane – TAC; The prices of cyclohexane, KA oil, and adipic acid are 1000 \$/ton, 2500 \$/ton, and 1800 \$/ton, respectively.

Scheme 2. Reaction Scheme for Benzene Chlorination

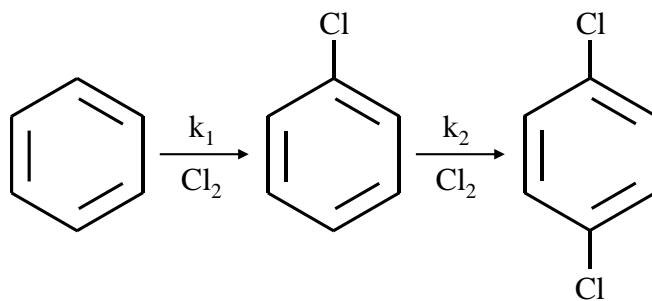


Figure 7. Initial superstructure for the benzene chlorination process

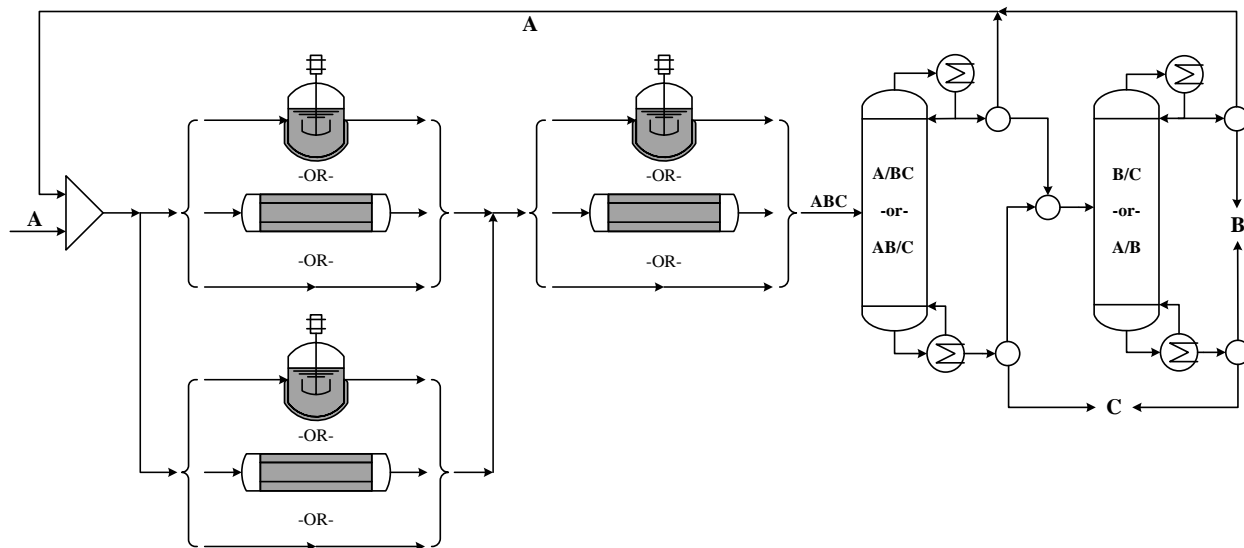


Figure 8. Optimal process configuration for the second case study (flowrate in kmol/h)

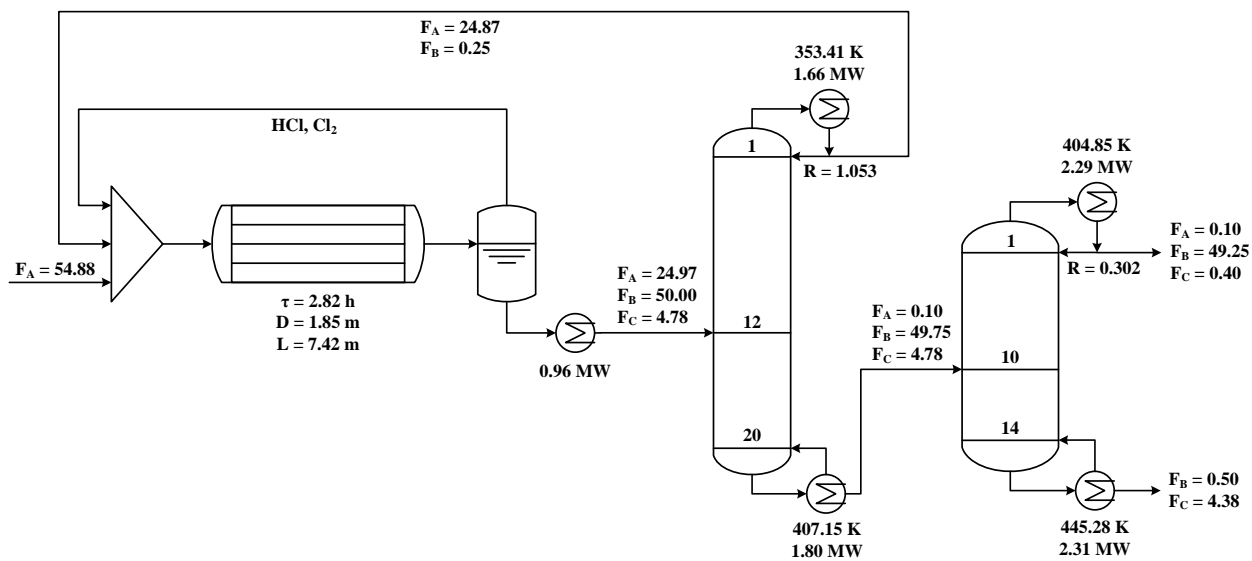


Table 4. Computational Results for the Benzene Chlorination Case Study

Optimal TAC (\$/year)	6.24×10^5
TAC in the first relaxed NLP (\$/year)	2.20×10^5
Number of equations	2490
Number of discrete variables	86
Number of variables	1784
Number of nonlinear matrix entries	2405
Code length	5916
Searched SBB nodes	167
Infeasible nodes	71
CPU time (s)	72

Table 5. Economic Optimization Results for the Benzene Chlorination Case Study

	Capital Investment (10 ⁵ \$/year)	Operational Cost (10 ⁵ \$/year)
Reactor	1.46	0.81
Heat exchanger	0.08	0.36
1 st Distillation column	0.91	0.75
2 nd Distillation column	0.87	1.00

Table 6. Comparison between Our Design Results and the Reference Design for the Benzene Chlorination Case Study

	Reference Design	Our Design
Reactor network	one PFR	one PFR
Input flowrate (kmol/h)	105.26	79.74
Reaction conversion	50%	69%
Reaction selectivity	95%	91%
Separation sequence	Direct separation	Direct separation
Feed location in the 1 st column	8	12
Number of trays in the 1 st column	16	20
Reflux ratio of the 1 st column	0.65	1.05
Feed location in the 2 nd column	6	10
Number of trays in the 2 nd column	14	14
Reflux ratio of the 2 nd column	0.15	0.30
TAC (\$/year)	6.26×10^5	6.24×10^5
Process profit (million \$/year)*	42.1	44.0

*Process profit = revenues of chlorobenzene and dichlorobenzene – cost of benzene – TAC; The prices of benzene, chlorobenzene, and dichlorobenzene are 800 \$/ton, 1450 \$/ton, and 1200 \$/ton, respectively.